AD-A101 013 CITY COLL NEW YORK F/G 17/2.1
ACQUISITION, IMAGE AND DATA COMPRESSION.(U)
APR 81 D L SCHILLING, G EICHMANN AFOSR-77-3217
UNCLASSIFIED 5137-4 AFOSR-TR-81-0536 NL

1 OF 1
AD
A101013

END
DATE
FILMED
7 81
DTIC

AFOSR-TR- 81 -0536

LEVEL

(12)

AD A101013

ACQUISITION, IMAGE AND DATA COMPRESSION

Final Scientific Report - 5137-4

March 1, 1977 - February 28, 1981

AIR FORCE OFFICE OF SCIENTIFIC RESEARCH

Bolling Air Force Base

Washington, D. C. 20332

Donald L. Schilling
Professor
Co-Principal Investigator

George Eichmann
Professor
Co-Principal Investigator

DEPARTMENT OF ELECTRICAL ENGINEERING

DTIC
ELECTE
JUL 7 1981
G

DTIC FILE COPY

THIS DOCUMENT IS BEST QUALITY PRACTICABLE.
THE COPY FURNISHED TO DDC CONTAINED A
SIGNIFICANT NUMBER OF PAGES WHICH DO NOT
REPRODUCE LEGIBLY.

THE CITY COLLEGE OF
THE CITY UNIVERSITY of NEW YORK

Approved for public release;
distribution unlimited.

81 7 06 009

DISCLAIMER NOTICE

THIS DOCUMENT IS BEST QUALITY PRACTICABLE. THE COPY FURNISHED TO DTIC CONTAINED A SIGNIFICANT NUMBER OF PAGES WHICH DO NOT REPRODUCE LEGIBLY.

UNCLASSIFIED

SECURITY CLASSIFICATION OF THIS PAGE (When Data Entered)

(12) 56

(19) REPORT DOCUMENTATION PAGE

READ INSTRUCTIONS BEFORE COMPLETING FORM

1. REPORT NUMBER: (18) AFOSR-TR-81-0536

2. GOVT ACCESSION NO.: AD-A101013

3. RECIPIENT'S CATALOG NUMBER

4. TITLE (and Subtitle): (6) ACQUISITION, IMAGE AND DATA COMPRESSION.

5. TYPE OF REPORT & PERIOD COVERED: Final Scientific Report, March 1, 1977 - Feb. 28, 1981

6. PERFORMING ORG. REPORT NUMBER

7. AUTHOR(s): (10) Donald L. Schilling, George Eichmann

8. CONTRACT OR GRANT NUMBER(s): AFOSR-77-3217

9. PERFORMING ORGANIZATION NAME AND ADDRESS: City College of New York, New York, N. Y. 10031

10. PROGRAM ELEMENT, PROJECT, TASK AREA & WORK UNIT NUMBERS: 61102F, (16) 2305/B1 (17) C1

11. CONTROLLING OFFICE NAME AND ADDRESS: Air Force Office of Scientific Research/NE, Bolling, AFB, Washington, D. C. 20332

12. REPORT DATE: April 15, 1981

13. NUMBER OF PAGES: 53

14. MONITORING AGENCY NAME & ADDRESS (if different from Controlling Office): (9) Final rept. 1 Mar 77 - 28 Feb 81

15. SECURITY CLASS. (of this report): UNCLASSIFIED

15a. DECLASSIFICATION/DOWNGRADING SCHEDULE

16. DISTRIBUTION STATEMENT (of this Report)

APPROVED FOR PUBLIC RELEASE; DISTRIBUTION UNLIMITED

(11) 15 Apr 81 (14) 51374

17. DISTRIBUTION STATEMENT (of the abstract entered in Block 20, if different from Report)

18. SUPPLEMENTARY NOTES

19. KEY WORDS (Continue on reverse side if necessary and identify by block number)

Spread Spectrum, Multiple Access, Optical Transforms, Acquisition, Delta Modulation, Simulation.

20. ABSTRACT (Continue on reverse side if necessary and identify by block number)

This report discusses four topics:

1) Operation of a frequency acquisition aid to acquire a direct sequence or frequency hopped signal. The acquisition aid employed is a FFT, and repeated measurements are employed to reduce the probability of error;

2) Multiple access using dynamic reservations. Here a new multiple access technique is described in which reservations are made which indicate whether the

DD FORM 1 JAN 73 1473 EDITION OF 1 NOV 65 IS OBSOLETE S/N 0102-014-6601

UNCLASSIFIED 084000

SECURITY CLASSIFICATION

(Cont.)

20. number of packets to be transmitted is to be increased or decreased. This technique is compared to the generally used procedure of indicating in the reservation the exact number of packets to be sent, a technique which requires significantly more bandwidth.

(12)

ACQUISITION, IMAGE AND DATA COMPRESSION

Final Scientific Report - 5137-4

March 1, 1977 - February 28, 1981

AIR FORCE OFFICE OF SCIENTIFIC RESEARCH

Bolling Air Force Base

Washington, D.C. 20332

Donald L. Schilling
Professor
Co-Principal Investigator

George Eichmann
Professor
Co-Principal Investigator

DEPARTMENT OF ELECTRICAL ENGINEERING

DTIC
ELECTE
JUL 7 1981
S C

Accession For
NTIS GRA&I ☑
DTIC TAB ☐
Unannounced ☐
Justification
By
Distribution/
Availability Codes
Dist | Avail and/or Special
A | 23

AIR FORCE OFFICE OF SCIENTIFIC RESEARCH (AFSC)
NOTICE OF TRANSMITTAL TO DDC
This technical report has been reviewed and is approved for public release IAW AFR 190-12 (7b).
Distribution is unlimited.
A. D. BLOSE
Technical Information Officer

Unc.

SECURITY CLASSIFICATION OF THIS PAGE (When Data Entered)

REPORT DOCUMENTATION PAGE		READ INSTRUCTIONS BEFORE COMPLETING FORM
1. REPORT NUMBER AFOSR-TR- 81 -0536	2. GOVT ACCESSION NO AD-A101013	3. RECIPIENT'S CATALOG NUMBER
4. TITLE (and Subtitle) ACQUISITION, IMAGE AND DATA COMPRESSION		5. TYPE OF REPORT & PERIOD COVERED Final Scientific Report March 1, 1977 - Feb. 28, 1981
		6. PERFORMING ORG. REPORT NUMBER
7. AUTHOR(s) Donald L. Schilling George Eichmann		8. CONTRACT OR GRANT NUMBER(s) AFOSR 77-3217
9. PERFORMING ORGANIZATION NAME AND ADDRESS City College of New York New York, N. Y. 10031		10. PROGRAM ELEMENT, PROJECT, TASK AREA & WORK UNIT NUMBERS 61102F 2305/B1
11. CONTROLLING OFFICE NAME AND ADDRESS Air Force Office of Scientific Research NE Bolling, AFB, Washington, D. C. 20332		12. REPORT DATE April 15, 1981
		13. NUMBER OF PAGES 53
14. MONITORING AGENCY NAME & ADDRESS (if different from Controlling Office)		15. SECURITY CLASS. (of this report) UNC
		15a. DECLASSIFICATION/DOWNGRADING SCHEDULE

16. DISTRIBUTION STATEMENT (of this Report)

Approved for public release; distribution unlimited.

17. DISTRIBUTION STATEMENT (of the abstract entered in Block 20, if different from Report)

18. SUPPLEMENTARY NOTES

19. KEY WORDS (Continue on reverse side if necessary and identify by block number)

Spread Spectrum, Multiple Access, Optical Transforms, Acquisition, Delta Modulation, Simulation.

20. ABSTRACT (Continue on reverse side if necessary and identify by block number)

This report discusses four topics:

1) Operation of a frequency acquisition aid to acquire a direct sequence or frequency hopped signal. The acquisition aid employed is a FFT, and repeated measurements are employed to reduce the probability of error;

2) Multiple access using dynamic reservations. Here a new multiple access technique is described in which reservations are made which indicate whether the

DD FORM 1 JAN 73 1473 EDITION OF 1 NOV 65 IS OBSOLETE S/N 0102-014-6601

UNCLASSIFIED

SECURITY CLASSIFICATION OF THIS PAGE

Number 20 continued:

number of packets to be transmitted is to be increased or decreased. This technique is compared to the generally used procedure of indicating in the reservation the exact number of packets to be sent, a technique which requires significantly more bandwidth.

3. HYBRID WHITE-LIGHT REFLECTIVE TRANSFORM PREPROCESSOR FOR REAL-TIME DIGITAL COLOR IMAGE TRANSMISSION

Signal-dependent noise encountered when sampling video signals at low sampling rate, while using an adaptive video deltamodulator both as an encoder and a video digitizer, is combated by using a white-light reflective transform optical preprocessor. While the white-light preprocessor works on black and white images, its main advantage is that it can simultaneous process using a single source, many color channels. Further, the relative lack of both spatial and temporal coherence aids in reducing speckle and interference noise effects. Color video images that have been preprocessed using this white-light optical preprocessor and then sampled close to their Nyquist rate are presented.

4. SUPERRESOLVING IMAGE RESTORATION OF NOISY IMAGES

Superresolving image restoration (SIR) in the presence of a noisy environment is considered. Most SIR algorithms, even in the absence of noise, can only resolve two point sources one-half Rayleigh distance apart. In this report, it is shown that in the absence of noise the SIR of two point source spaced one-eighth of a Rayleigh distance apart is possible. The algorithms use optimal noise filtering techniques based on the methods of linear programming. For noisy images, the combination of linear eigen-value and optimal noise filtering is used. In this report, it is shown that for a diffraction-limited image of two point sources spaced one-half Rayleigh distance apart, whose input signal-to-noise ratio is 21db, SIR is achievable. These results have important implications in atmospheric optics, seismology, radio astronomy, medical diagnostics and digital bandwidth compression applications where the deconvolution of noisy bandwidth-compressed images is one of the fundamental limitations.

Table of Contents

	Page
I. Research Objectives	1
II. Status of the Research Effort	2
III. Professional Staff	47
IV. Papers Published	48

I. Research Objectives

1. Frequency Acquisition of a Spread Spectrum Signal

The Phase Locked Loop (PLL) is a device which uses the principle of negative feedback to provide and maintain a reference point required to obtain the information contained in the received signal. Usually this reference point is the carrier frequency of the received signal. In practical systems the received signal is at an unknown frequency located within a specified relatively wide bandwidth. To acquire the signal, the PLL is designed to have a narrow bandwidth which precludes rapid acquisition. To significantly reduce the acquisition time one can employ an "acquisition aid".

The acquisition aid studied under this grant employs the Fast Fourier Transform (FFT). It is shown that this technique greatly enhances the acquisiton capability of a PLL system operating in the presence of noise.

2. Multiple Access using Dynamic Reservations

The need for a multiaccess protocol arises whenever a resource is shared by many independent contending users. Two major factors contribute to such a situation: (a) the need to share expensive resources in order to achieve their efficient utilization, and (b) the need to provide a high degree of convectivity for communication among independent users.

The multiaccess scheme studied under this grant combines a dynamic allocation reservation technique with conventional time division multiple access to provide a system in which the delay time is minimized for a given throughput.

3. Hybrid White-Light Reflective Transform Preprocessor for Real-Time Digital Color Image Transmission

Image processing for the purpose of digital bandwidth compression of video images transmitted in a real-time environment is pursued.

4. Superresolving Image Restoration of Noisy Images

Reconstruction of objects that have been degraded by limited bandwidth channels is studied.

II. Status of the Research Effort

1. Frequency Acquisition of a Spread Spectrum System

Our research is concerned with the use of an acquisition aid which derives an "aiding" signal via a FFT processing of the incoming signal. The scheme utilizes an iterative technique, so that by detecting the center frequency of the received signal, we can decrease the uncertainty band or frequency window within which the center frequency presently resides. When the uncertainty band is small enough compared to the final desired phase locked loop (PLL) bandwidth B_L, a narrow tracking loop can be switched in to complete the locking procedure.

The possible implementations of the acquisition aid in the PLL or in the Costas loop are shown in Fig. 1 and Fig. 2 respectively. Position A of the switches, shown on these figures, is used during acquisition, while position B is used to track the incoming signal once acquisition is obtained.

The center frequency of the received signal may have a shift with respect to the transmitter's signal frequency due to the transmitter's oscillator instabilities and/or a Doppler shift. We shall group the total of all these variations into one and refer to it as the Doppler shift Δf_D. Furthermore, we will assume that the Doppler shift is slowly varying and may, therefore, be considered constant during the acquisition process. Because of the Doppler shift, the center frequency of the received signal is known only to lie in a practicular frequency window Δf_{W1} (Fig. 3), where

$$\Delta f_{W1} = f_H - f_L \tag{1}$$

and the received signal is sampled at the sampling intervals

$$T_{S1} = \frac{1}{2 \Delta f_{W1}} \tag{2}$$

After sampling the received signal N_1 times, the acquisition aid

calculates an N_1 - point FFT of it. The frequency resolution obtained by the N_1 - point FFT is

$$f_{R1} = \frac{1}{N\,T_{S1}} \tag{3}$$

and substituting Eq. 2 into Eq. 3 we obtain

$$f_{R1} = \frac{2\,\Delta f_{W1}}{N} \tag{4}$$

In the time domain we have N_1 sampled points T_{S1} sec. apart, and in the frequency domain we have N_1 points f_{R1} Hz. apart, or equivalently N_1 filters, each of them with a bandwidth of f_{R1} Hz.

As a possible implementation for the acquisition aid we select as the received signal's center frequency, the one at which occurs the maximum of the magnitude-squared of consecutive complex N_1 - point FFT. The time required to acquire will then be

$$T_{ACQ} = N_1 T_{S1} \tag{5}$$

The probability P_c of choosing the correct frequency as the center frequency of the received signal is proportional to the ratio of the signal power P_s to the noise power P_N in each filter:

$$P_C \sim \frac{P_S}{P_N} \tag{6}$$

where the noise power contained in each filter is

$$P_N = \frac{\eta}{N_1\,T_{S1}} \tag{7}$$

Substituting Eq. 7 in Eq. 6 we obtain the equation

$$P_C \sim \frac{P_S T_{S1} N_1}{\eta} \tag{8}$$

The digital signal used to generate the carrier's phase modulation uses a Non-Return-to-Zero (NRZ) format. It is readily shown that for this case 90% of the signal power is in the interval $\pm f_b$ Hz. around the received signal's center frequency (f_b is the bit rate of the NRZ signal) and 70% of the signal power is in the interval $\pm f_b/2$. If we reduce the filters' bandwidth by increasing N_1, we decrease the noise power contained in each filter but, at bandwidths less than f_b, the signal power in the filter is reduced as rapidly as the noise power. There is therefore no improvement in the probability of choosing the correct frequency by reducing the filters' bandwidth below f_b and in our computer simulations of the acquisition aid we used f_b as the filter bandwidth.

To increase P_C, we use an iterative technique by which we effectively increase the signal-to-noise ratio. As before we calculate an N_1 - point FFT of the N_1 - sampled points but we store in the processor's memory the magnitude-squared of the consecutive complex $N_1/2$ - point FFT. Then, the scheme performs a second calculation of the magnitude-squared of consecutive, complex $N_1/2$ - point FFT of a new set of independent N_1 sampled points and it adds point-by-point the resulting magnitudes to the magnitudes stored in the memory.

To lower the probability of selecting an incorrect frequency as the center frequency of the received signal, we may need several iterations, depending on signal-to-noise ratio. However, this process is limited by the time of acquisition required by the system in the acquisition mode. In general, however,

$$T_{ACQ} = K N_1 T_{S1} \tag{9}$$

where K is the number of iterations.

Once the iterations of the FFT's magnitude-squared calculations and their additions are completed, the scheme finds the maximum value of the resulting $N_1/2$ numbers stored in memory, and it uses the frequency at which the maximum appears to move the center frequency of the receiver's Voltage Controlled Oscillator.

Substituting Eq. 2 in Eq. 9 we obtain as the acquisition time required by the scheme

$$T_{ACQ} = \frac{K N_1}{2 f_{W1}} + T_{CALC} \tag{10}$$

where T_{CALC} is the time required by the scheme to calculate the FFTs, magnitudes-squared, and additions.

We present, in Fig. 4, plots of the probability of selecting incorrect frequency P_e as a function of the signal-to-noise ratio E_b/η, and the parameters λ, which is the ratio of the filters' bandwidth, f_{R1}, to the signal bit rate, f_b.

$$\lambda = \frac{f_{R1}}{f_b} \tag{11}$$

The computer simulation made only one FFT calculation, choosing the frequency of the maximum of the set of the magnitude-squared of the $N_1/2$ consecutive, complex, numbers, as the signal's center frequency.

On Figs 5 and 6, we show the results in the case of two iterations, $K = 2$, and three iterations, $K = 3$, respectively. Note that for probabilities of error less than 0.1, $\lambda = 1$, is optimum, i.e., the filter bandwidth should be chosen to be equal to the bit rate f_b.

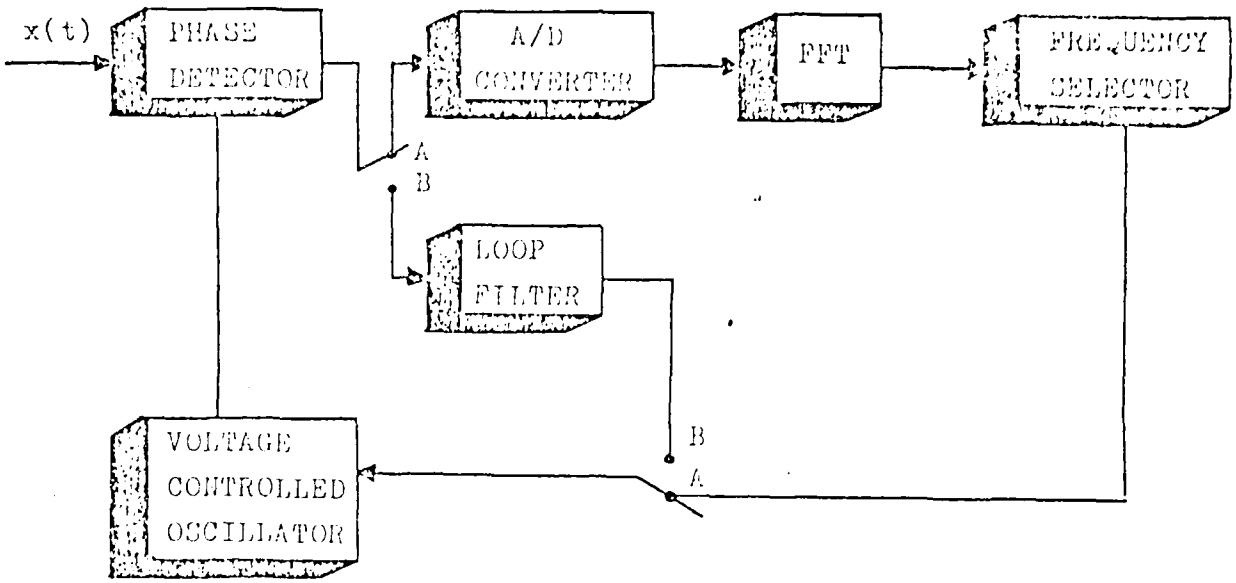

Fig.1 Phase Locked Loop With Proposed Acquisition Aid.

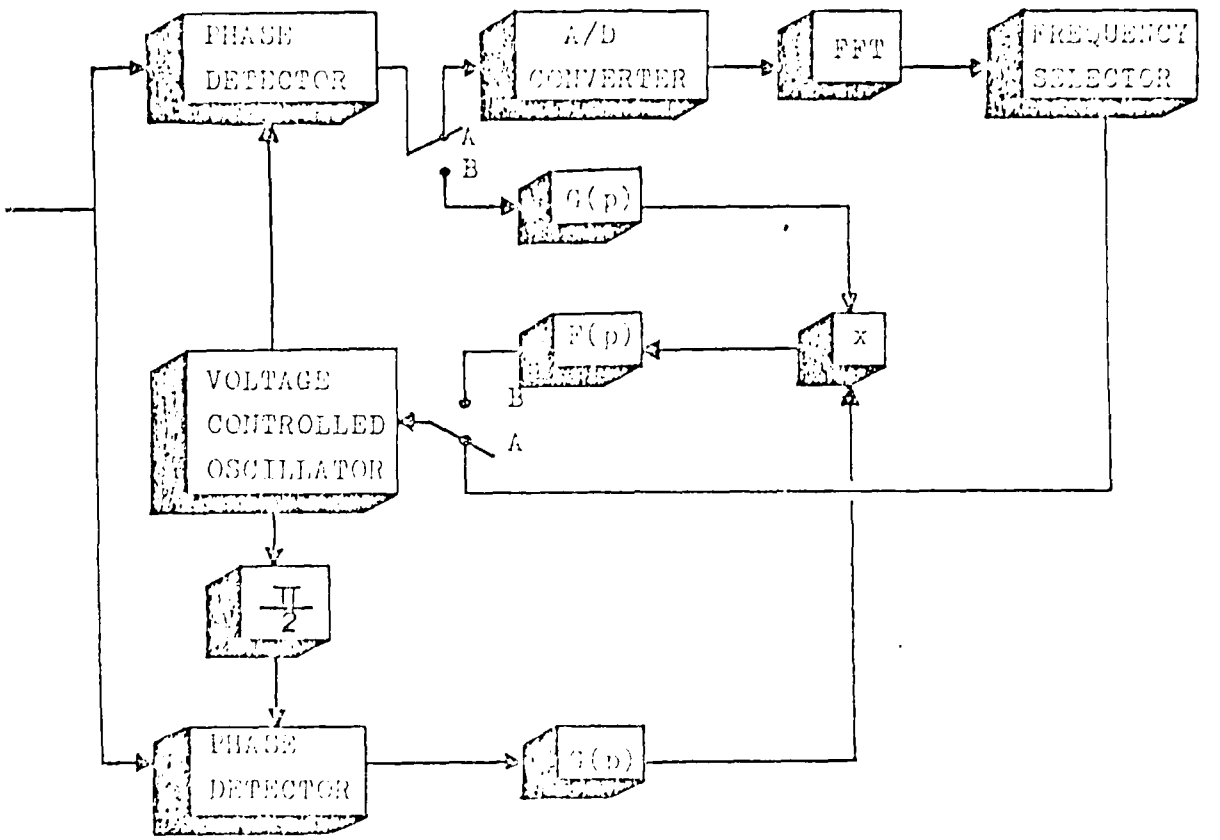

Fig. 2 The Costas Loop With Proposed Acquisition Aid.

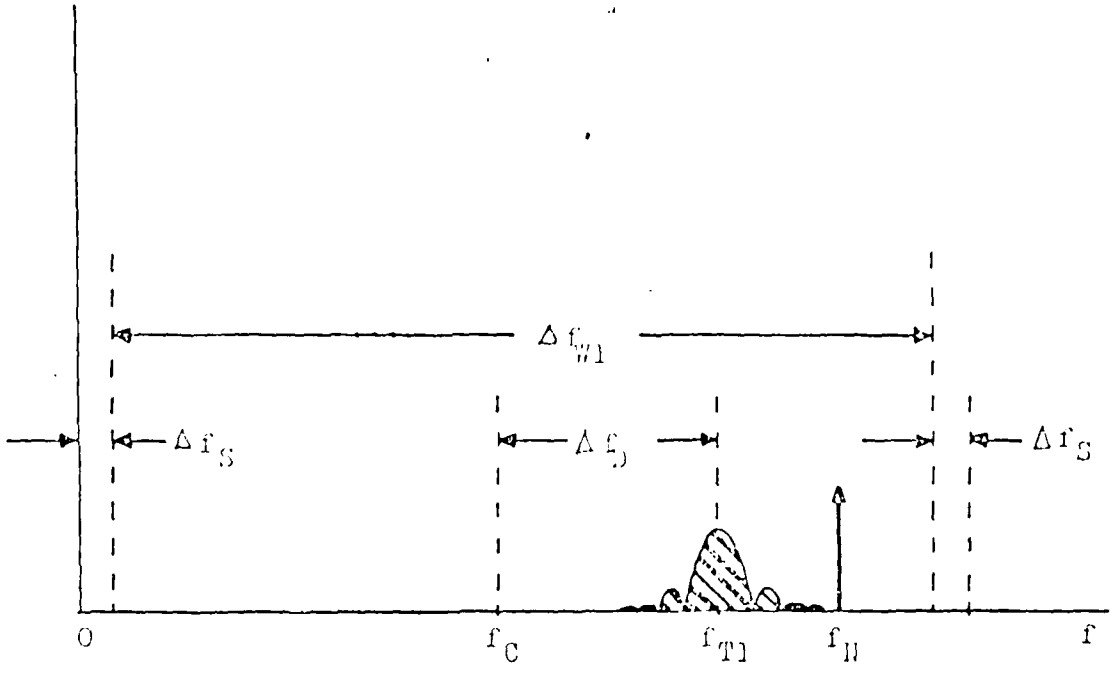

Fig.3 Spectrum of Signal During First Iteration of Acquisition Aid.

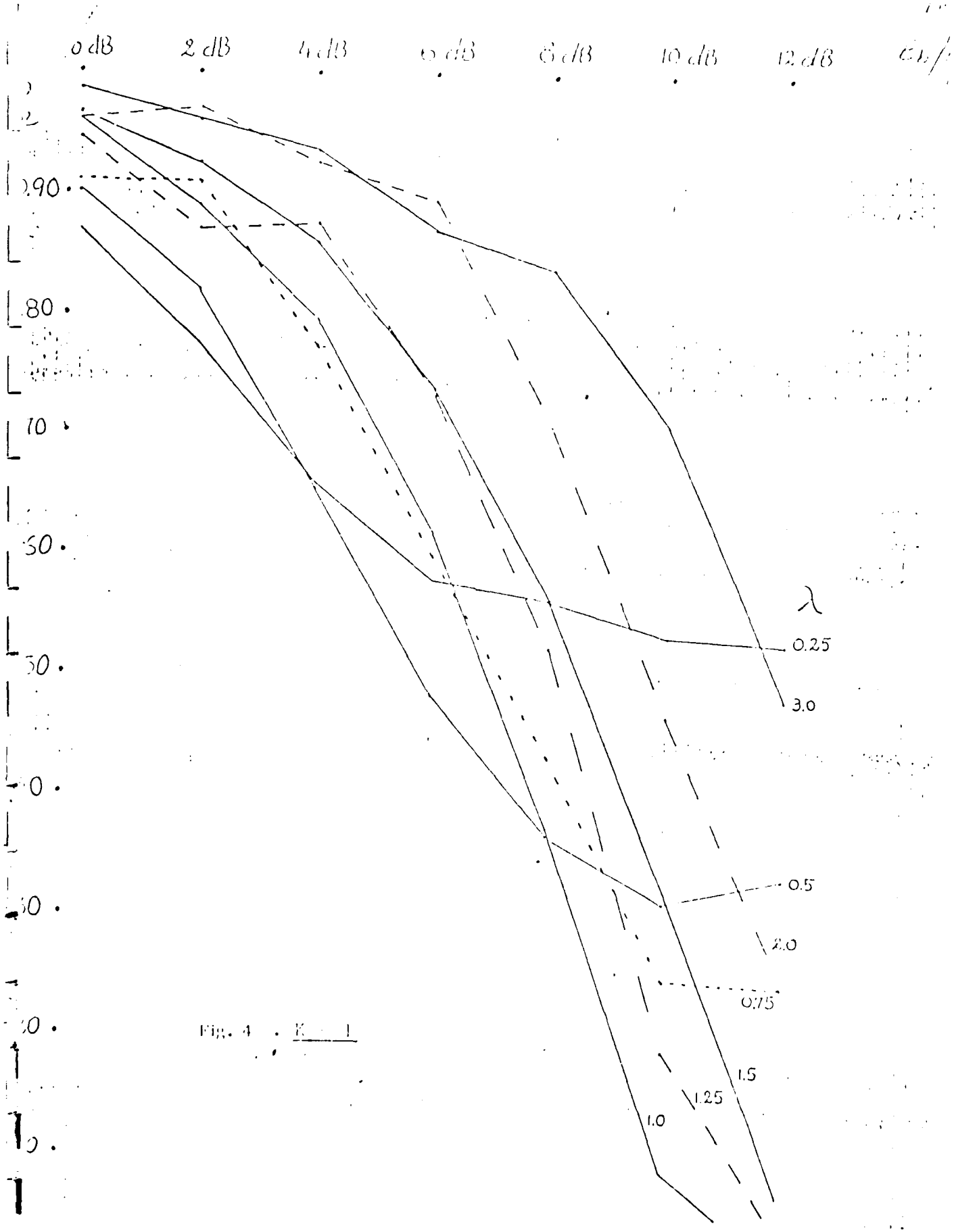
0 dB
2 dB
4 dB
6 dB
8 dB
10 dB
12 dB
.90
.80
.70
.60
.50
.40
.30
.20
.10
λ
0.25
3.0
0.5
2.0
0.75
1.5
1.25
1.0

Fig. 4 . K = 1

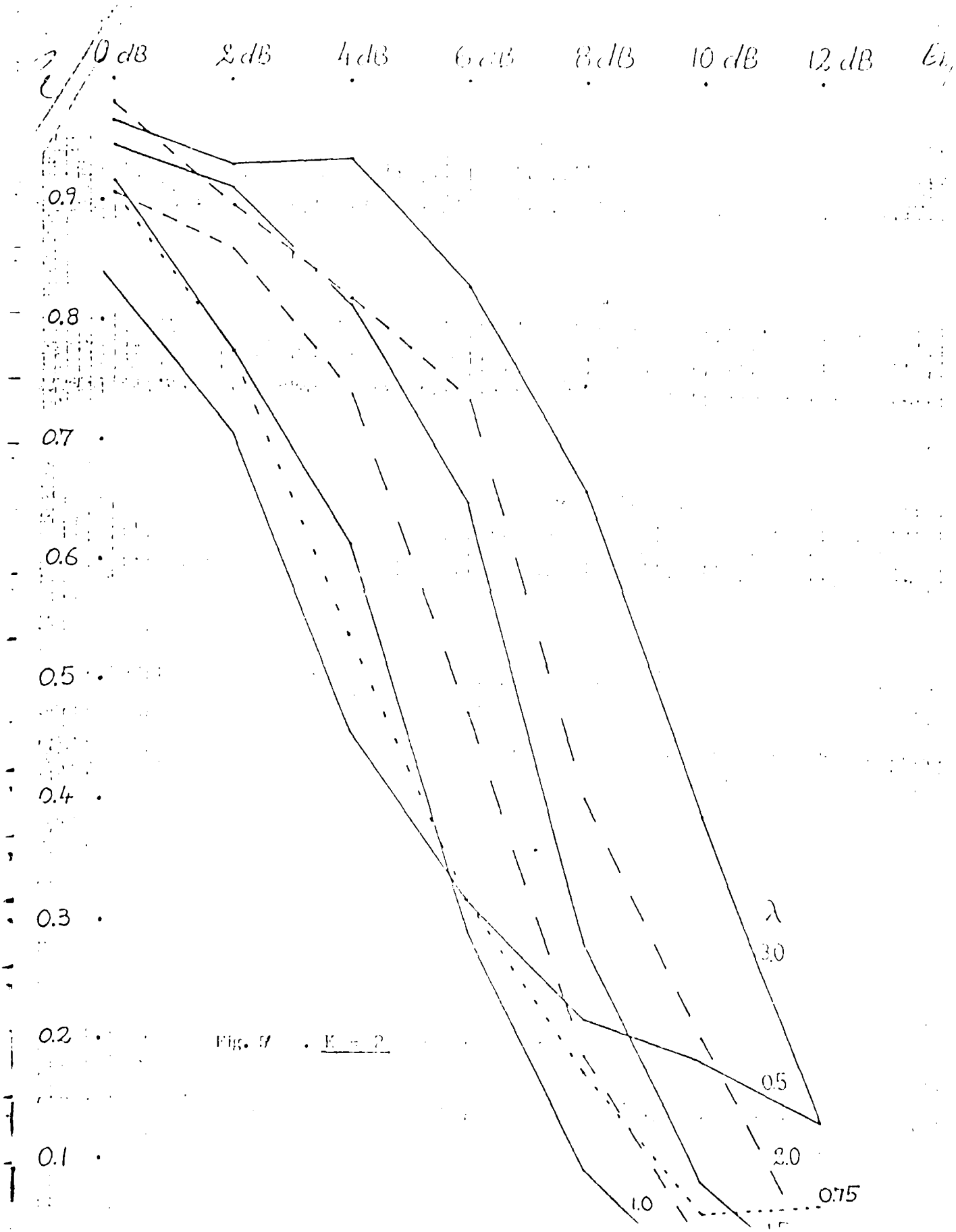
0 dB
2 dB
4 dB
6 dB
8 dB
10 dB
12 dB
0.9
0.8
0.7
0.6
0.5
0.4
0.3
0.2
0.1
λ
3.0
0.5
2.0
0.75
1.0

Fig. 9 . E = 2

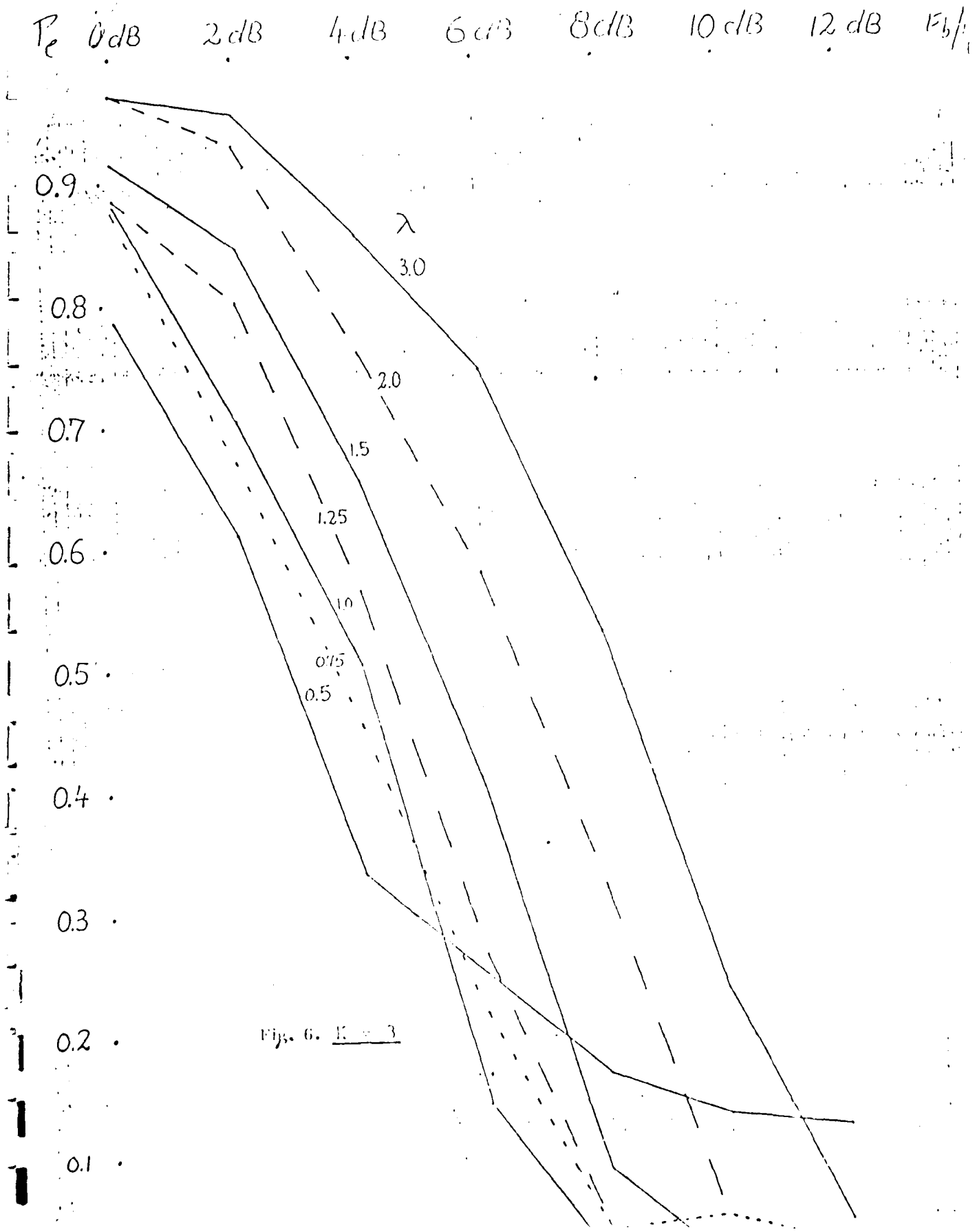
P_e
0dB
2dB
4dB
6dB
8dB
10dB
12dB
E_b/N_0
0.9
0.8
0.7
0.6
0.5
0.4
0.3
0.2
0.1
λ
3.0
2.0
1.5
1.25
1.0
0.75
0.5

Fig. 6. K = 3

2. Multiple Access using Dynamic Reservations

Our proposed scheme consists of a dynamic time-assignment system which retains the allocation fairness while allowing nodes to make use of channel capacity otherwise wasted due to light traffic loads and/or a nonuniform distribution of traffic among the nodes. In particular, it allows shorter messages to be sent with delays very close to those encountered when using only fixed TDMA, while at the same time allowing longer messages to use more channel capacity.

In this proposed scheme, time is divided into frames, each consisting of one slot (for reservations and acknowledgments) and Reserved Time Slots for reserved data packets. The number of the Reserved Slots will vary, depending on the demand of the stations as illustrated below.

Each station will send two bits (0, 0) (or only 0 in this case), (0, 1), or (1, 1) into the reservation slot which is divided into 2N small slots, where N is the number of stations. The (0, 0) vector represents that the station does not have any packet for transmissions, the (0, 1) vector represents that the station has only one packet to transmit, and the (1, 1) vector represents that the station has two or more packets to transmit. One major advantage of this scheme is seen to be that the reservation time is a very small percentage of the total frame time, which is not true for other existing schemes. The data packets waiting at the stations will be transmitted into Reserved Slots of the frame, whose number will vary according to the following rules:

a) There will be no time slot reserved for the station which has sent the (0, 0) vector;

b) There will be one time slot reserved for transmission for the station which has sent the (0, 1) vector;

c) The station which has sent the (1, 1) vector will be allotted time slots (equal to or greater than two) which will depend on its prior reservation vectors as follows:

i) Two (2) slots will be reserved for transmission if the first preceding reservation vector is (0, 0) or (0, 1); in other words if the second bits in the present and the first preceding vector forms (0, 1).

ii) P time slots where P is equal to or greater than two will be reserved for transmission if the first preceding vector is (1, 1) but the second preceding vector is (0, 0) or (0, 1); in other words if the second bits in the present and the preceding two vectors form (0, 1, 1).

iii) Q time slots where Q is equal to or greater than P will be reserved for transmission if the preceding two vectors are both (1, 1); in other words if the second bits in the present and the preceding two vectors for (1, 1, 1).

Preliminary Simulation Results

A FORTRAN simulation program was written to find the behavior of the system. An exponential interarrival time distribution was used for each user with separately defined means. A 10-node, 50 kbps channel was used. Traffic was equal distributed among the nodes. The abscissa is the average total packet delay for all nodes and includes all queueing, transmission, and propagation times. The ordinate is total channel throughput due to traffic from all nodes, when throughput includes overhead bits.

The results for two other schemes are also shown in comparison in Fig. 1. The curves for Robert's scheme[1] and Binder's scheme[2] represent analytical results. Different values of P and Q are considered in our simulation program. As can be seen from Fig. 1, the proposed Round-Robin dynamic scheme gives a significant improvement for short packet delay over the other reservation schemes.

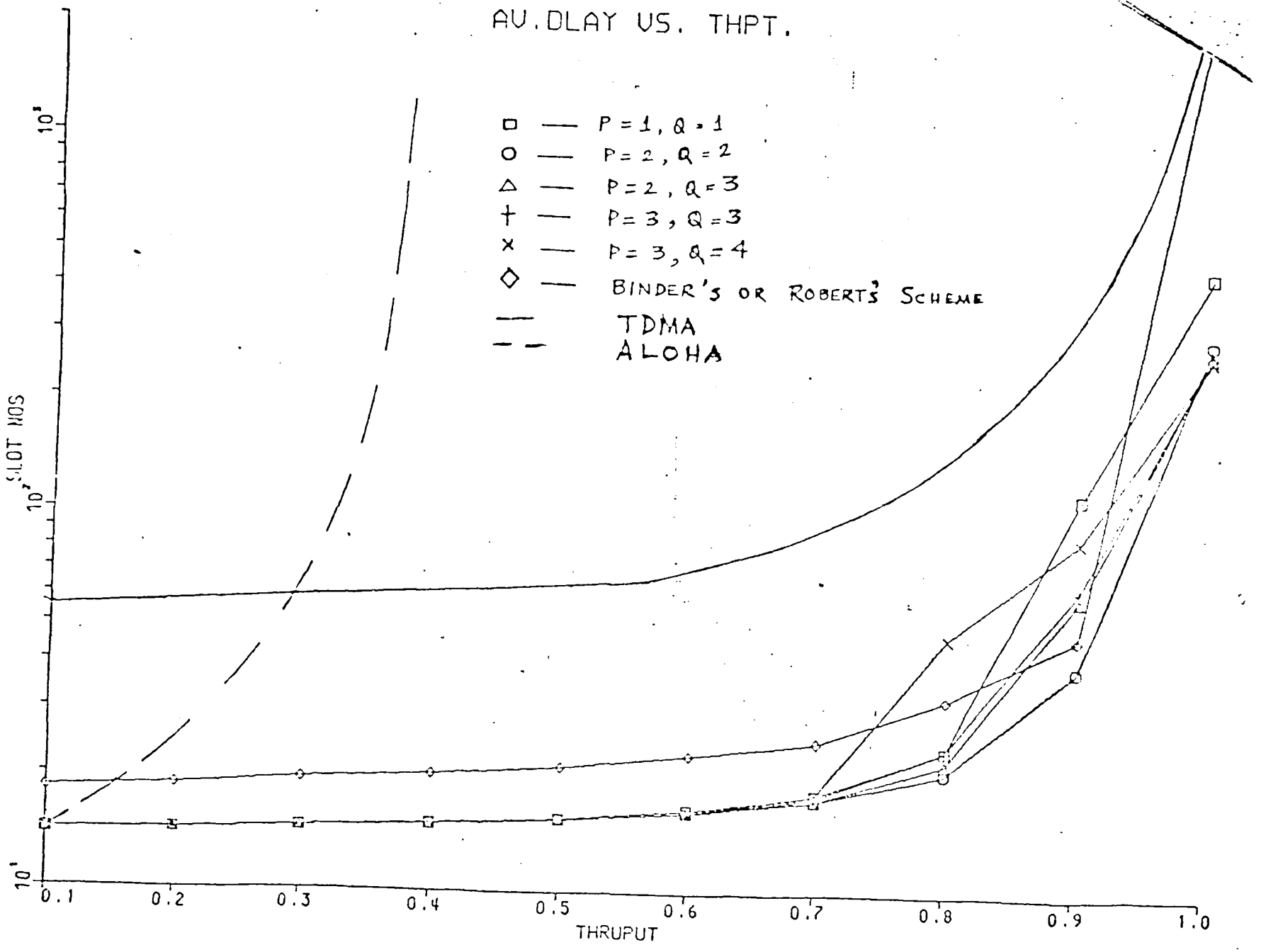
AV. DLAY VS. THPT.
□ — P = 1, Q = 1
○ — P = 2, Q = 2
△ — P = 2, Q = 3
+ — P = 3, Q = 3
× — P = 3, Q = 4
◇ — BINDER'S OR ROBERTS' SCHEME
— TDMA
- - ALOHA
SLOT NOS
THRUPUT
0.1
0.2
0.3
0.4
0.5
0.6
0.7
0.8
0.9
1.0

REFERENCES

(1) L. G. Roberts and B. D. Wessler, "Computer Network Developments to achieve resource sharing", *in 1970 Spring Joint Comput. Conf.*, Proc. AFIPS Conf., vol. 36, 1970, pp. 543-549.

(2) I. M. Jacobs, R. Binder, and E. V. Hoversten, "General Purpose Packet Satellite Networks", Proc. IEEE, vol. 66, Nov. 1978.

3. HYBRID WHITE-LIGHT REFLECTIVE TRANSFORM PREPROCESSOR FOR REAL-TIME DIGITAL IMAGE TRANSMISSION

INTRODUCTION

Along with the development of sophisticated monitoring and communication equipment the need for real-time video image transmission is apparent. Digital signal transmission offers many advantages over analog transmission when operating over a channel that is corrupted by noise. This is due to the fact that quantized levels are more easily discriminated from the effects of noise. In addition, the digital format allows for time multiplexing, error-coding as well as encrypting procedures that are not available on an analog channel. However, when the standard four MHz video signal is sampled at the Nyquist rate and encoded using pulse code modulation to four to six quantization levels, the data rate becomes 48-64 Mbs. In the case of color video signals, it is not uncommon to require 85-90 Mbs digital bandwidth for color PCM encoded digital video rates. This high digital bandwidth is usually unacceptable in many applications. Various digital encoding alternatives have been explored to reduce the digital bandwidth to an acceptable level. One such solution is a hard-wired adaptive deltamodulator that works at video rates. This solution is explored in this report. In order to compress the digital bandwidth it is necessary to operate the ADM close to its Nyquist rate. However, when an ADM runs near its Nyquist rate a new noise source, and effect that is signal dependent and is termed edge busyness, appears. This noise source is due to the adaptive property of the ADM leading to oscillatory behaviour near the Nyquist rate. For an ADM this noise source is the fundamental limitation in reducing the digital video bandwidth.

In an ADM, the step size algorithm is signal dependent. Due to different initial conditions, scanning from line to line, as well as frame to frame, a vertical edge encountered in the image, will occur at different positions in the scan. As the sampling rate is decreased, the error between the steps, and especially near the edges, increases. At low sampling rate the edge seems to "wiggle" about a vertical line. This noise not only degrades image quality, but it also leads to operator fatigue. To reduce edge busyness, the allowable slope overload must be reduced. The slope overload is usually reduced by passing the video signal through a low pass filter. However, when operating the ADM close to the Nyquist rate, which is inversely proportional to the cut-off frequency of the low pass filter, additional artifacts will occur. A two dimensional preprocessing of the video image for the purpose of reducing the possible slope overload of the ADM is an alternative explored in this report.

WHITE-LIGHT HYBRID PROCESSOR

Highly coherent analog spatial transform processors suffer the disadvantage that they are sensitive to positional tolerance error, dirt noise on the lenses as well as problems with speckle noise. By decreasing the spatial coherence of the transform processor some of these objections can be circumvented. It is known that an incoherent source, such as an arc lamp, can acquire spatial coherence by passing its output through a pinhole. In this case, the light appears to emanate from a single point source. The light radiating from the pinhole has a weaker intensity, compared to laser source, and its region of spatial coherence is rather restricted. However, using a low light level detector and re-

stricting the size of the input transparency these problems can be overcome. The purpose of this section is to report on a white-light transform image bandwidth compressor.

The arrangement for the white-light transformer follows the physical layout of a fully coherent narrowband optical transform processor. The source used in this experiment is a broadband 200 W Mercury-Xenon arc lamp source. The arc source output is first spatial filtered by focusing its output on a pinhole. The size of the pinhole, 0.37mm diameter used for our experiment, was chosen as a compromise between a small pinhole that would block most of the light as well as create a chromatic diffraction pattern and a larger pinhole that would restrict the region of lateral spatial coherence. The light form the pinhole is collimated by F/5 6" diameter lens. The angular spread of the collimated beam is inversely proportional to the lateral coherence length of the white-light transform system. Instead of the usual telescopic transform lens configuration, we have chosen a refractive transform system. The advantage of a refractive optics, for the usual high F number transform system, is that it can be more compact than its refractive counter part. Further, since a first surface mirror does not have chromatic aberration, this system is better suited for a white-light processor than chromatically-balanced telescopic lenses. There are two possible relective transform systems: a system that uses a single on-axis parabolic mirror or a system that uses two off-axis parabolic mirrors for transform and retransform. In the first configuration the spatial filter must be reflective, while in the second configuration it is the usual transmissive filter. In either case the object is mounted

off-axis and only half of the mirror is used for transform or retransform. While the off-axis mounting introduces an additional phase shift, for incoherent images such additional phase shift carries no information. In our experiment we used a single on-axis mirror. For this configuration the object, the transform and image are all formed in the focal plane of the mirror. The off-axis mounting helps to separate the three regions. In the series of figures the results of the preprocessed, sparsely sampled, video images are presented.

LIST OF ILLUSTRATIONS

Figure 1. Color Still Image using 20 Mbs/sec per color channel, no optical filtering.

Figure 2. Color Still Image using 20 Mbs/sec per color channel with optical filtering.

Figure 3. Color Moving Image using 10 Mbs/sec per color channel, vertically scanned without optical filtering. The stripe is due to the single reflex shutter.

Figure 4. Color Moving Image using 3.5 Mbs/sec per color channel, vertically scanned with optical filter.

Figure 5. Slowly-moving Color Image of Girl at 4.0 Mbs/sec per color channel without optical filtering.

Figure 6. Slowly-moving Color Image at 4.0 Mbs/sec per color channel with optical filtering.

FIGURE 1. COLOR STILL IMAGE USING 20 MBS/SEC PER COLOR CHANNEL, NO OPTICAL FILTERING.

FIGURE 2. COLOR STILL IMAGE USING 20 MBS/SEC PER COLOR CHANNEL WITH OPTICAL FILTERING.

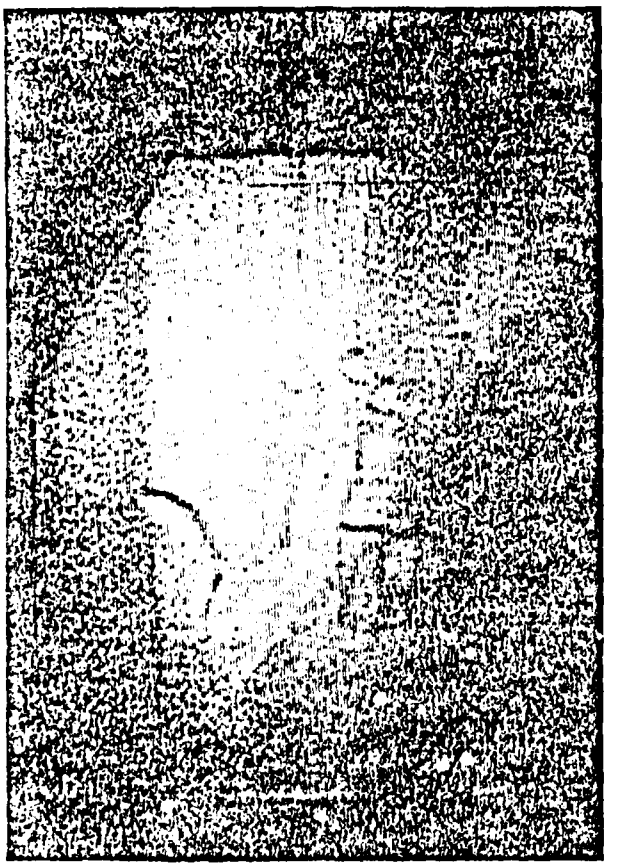

FIGURE 3. COLOR MOVING IMAGE USING 10 MBS/SEC PER COLOR CHANNEL, VERTICALLY SCANNED WITHOUT OPTICAL FILTERING. THE STRIPE IS DUE TO THE SINGLE REFLEX SHUTTER.

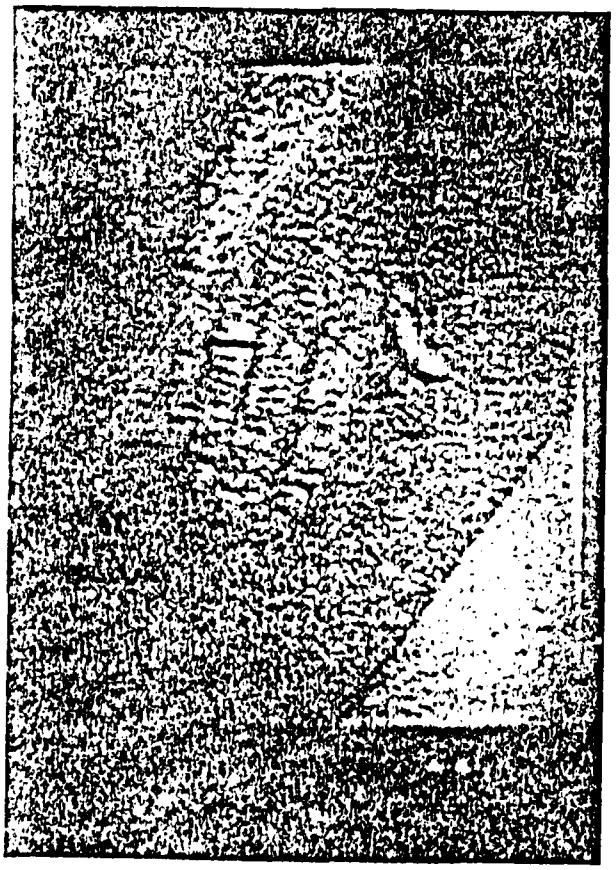

FIGURE 4. COLOR MOVING IMAGE USING 3.5 MHZ/SEC PER COLOR CHANNEL, VERTICALLY SCANNED WITH OPTICAL FILTER.

FIGURE 5. SLOWLY-MOVING COLOR IMAGE OF GIRL AT 4.0 MBS/SEC PER COLOR CHANNEL WITHOUT OPTICAL FILTERING.

FIGURE 6. SLOWLY-MOVING COLOR IMAGE AT 4.0 MBS/SEC PER COLOR CHANNEL WITH OPTICAL FILTERING.

4. SUPERRESOLVING IMAGE RESTORATION OF NOISY IMAGES

INTRODUCTION

The problem of restoring a linearly degraded image has been the subject of extensive investigations [1]. The mathematical formulation of the image restoration problem is common to many diverse fields such as atmospheric optics [2], seismology [3], spectroscopy [4], radio astronomy [5,6] as well as the general subject of numerical analysis [7]. In general, the inversion of linear degradation can be accomplished in a number of ways [1]. When the measurement error, that is the noise, is negligible and the degradation process is well-behaved, the direct inversion of the degradation process can easily be performed. For a well-conditioned degradation process, in the presence of noise, methods such as Wiener filtering are appropriate [8]. However, in many cases the degradation process is ill-conditioned. In this case the measurement errors are greatly amplified in the restoration leading to an image estimate that is dominated by noise. In this paper we discuss the restoration of ill-conditioned linearly degraded images that have been corrupted by appreciable noise.

While many types of ill-conditioned image restoration can be considered, a particular ill-conditioned image restoration, the restoration of a diffraction-limited image of finite extent has been used as a benchmark to compare the various restoration algorithms. Further, this model serves as a good starting point for the restoration of a severely bandwidth compressed video image. Such images are of interest in digital TV applications.

It has been shown [9,10] that for images of finite extent, in the absence of noise, spectral components of the signal that have been removed can be reconstructed from the low-passband information using analytic continuation. The extrapolation in the spatial frequency domain represents an increase in the spatial resolution

SUPERRESOLVING IMAGE RESTORATION OF NOISY IMAGES

ABSTRACT

Superresolving image restoration (SIR) in the presence of a noisy environment is considered. Most SIR algorithms, even in the absence of noise, can only resolve two point sources one-half Rayleigh distance apart. In this report, it is shown that in the absence of noise the SIR of two point source spaced one-eighth of a Rayleigh distance apart is possible. The algorithms use optimal noise filtering techniques based on the methods of linear programming. For noisy images, the combination of linear eigen-value and optimal noise filtering is used. In this report, it is shown that for a diffraction-limited image of two point sources spaced one-half Rayleigh distance apart, whose input signal-to-noise ratio is 21db, SIR is achievable. These results have important implications in atmospheric optics, seismology, radio astronomy, medical diagnostics and digital bandwidth compression applications where the deconvolution of noisy bandwidth-compressed images is one of the fundamental limitations.

in the spatial domain. An image restoration process which provides this increase in resolution is called a superresolving image restoration (SIR) process. A complete survey of recent SIR methods has been given by Frieden [1]. In general, statistical image restoration methods are not superresolving. Deterministic methods use various forms of regulatization [11] to provide stability for the image restoration. Linear shift-invariant filters, while they provide stability, are also not superresolving. It has been postulated that only non-linear filtering methods will provide SIR in the presence of noise [1]. The purpose, and the advance, of this paper is to show that the combination of linear shift-invariant filtering of the image and non-linear restoration does provide SIR capability in a realistic noise environment. The optimal noise filtering uses linear programming techniques. The linear programming method provides both cost and time effective ways to produce SIR.

FORMULATION

The SIR problem requires the inversion of a Fredholm integral equation of the first kind with a sampling function kernel. This kernel corresponds to coherent imaging. It is well-known that the incoherent band-limiting kernel has twice the spatial cut-off frequency as compared to the corresponding coherent sampling function kernel. Therefore, the coherent SIR is more stringent and thus provides a better benchmark than the corresponding incoherent kernel.

The discretized form of the image restoration problem can be formulated as a solution to the matrix linear equation

$$g = Hf + n \qquad [1]$$

where f,g are the sampled values of the restored (desired) diffraction-limited and the measured band-limited images, respectively n

is the sampled noise vector and H is a matrix representing the sinc integral operator obtained by using some appropriate quadrature rule. Therefore, f,g and n are N dimensional vectors while H is an NxN square matrix. The system of linear equations, represented by the matrix Eq.{1}, is undetermined since there are N equations and 2N unknowns. The unknowns are the components of the N dimensional vectors f and n. Neglecting the noise vector does not per se simplify the problem because for SIR the H, the degradation, matrix is nearly singular. Because of the singularity of the H matrix, the inverse H is highly unstable.

To stabilize the inverse H matrix, the eigen-values and the eigen-vectors of the inverse matrix are filtered. As it is known, the eigen-vectors of the H matrix are the discrete prolate spheroidal wave sequences {12}, the analog of the prolate spheroidal wavefunctions of the continuous case. The eigen-values of the H matrix, depending on the space-bandwidth product, vary between zero and unity. The high order eigen-sequences, corresponding to rapidly oscillating functions represent the eigen-values close to zero. The instability of the inverse matrix is due to near zero eigen-value of the H matrix. By filtering (attenuation) of these eigen-values of the H matrix, stable inverse matrix can be constructed. There are a number of filtering schemes that have been suggested both by us as well as others to do this filtering {13}. Some of these filtering schemes can be implemented using a real-time optical image processor. While these schemes do stabilize the inverse H matrix, since they tend to eliminate the high order eigen-values and precisely those eigen-values and eigen-vectors that contain the high spatial frequency information necessary for superresolution, they are not SIR methods. Further, since this method does not take into account the measurement errors, a critical factor in a highly unstable matrix inversion, other methods must be sought.

To obtain SIR additional information or constraints, must be utilized. Methods of image restoration that impose positivity constraints on

the restored image to obtain stability [14,15,16] have been described. We use positivity, boundedness, derivative constraints together with eigen-value filtering to obtain SIR. The additional filtering can be looked upon as optimal noise filters. This method of filtering can be formulated as a linear programming problem. In this formulation, the superresolving image is reconstructed subject to various optimality conditions. In this paper we shall use two minimum noise constraints, the so-called l_1 and l_∞ constraints. The l_1 constraint minimizes the linear sum of the positive and negative sample noise component values. The l_∞, also called minimax constraint, minimizes the maximum noise sample value. This sample value can either be positive or negative going sample noise value. Other noise performance criteria may also be used.

A figure of merit of the SIR is the Rayleigh distance. The Rayleigh distance is defined in terms of impulse response of two point sources. Two point sources separated by a Rayleigh distance in the absence of noise, will have their individual impulse responses arranged in such a way that the peak value of one source impulse response falls on the zero of the second source impulse response. With this definition, the combined impulse response has a double-humped appearance signifying the superposition of two individual source responses. The Rayleigh criteria can be related to the space bandwidth product of the system. Since the SIR is measured in terms of a Rayleigh criteria, it is customary to evaluate the SIR algorithm performance in terms of how well it resolves two neighboring point sources.

RESULTS AND CONCLUSIONS

The results are presented in a series of graphs. In each graph, the total two-sided spatial bandwidth is unity. By varying the spatial extent of the image, the space-bandwidth product and the corresponding effective Rayleigh distance is changed. In all of the examples, the total number of processed samples is thirty-two. This number allows the replacement of the cumbersome discrete Fourier transform (DFT) with the computationally more efficient fast Fourier transform (FFT) algorithm. The image to be reconstructed is a diffraction-limited image of two impulses. The two impulses are represented on the graph by one sampling point each separated by two samples. Because the way the graphics package draws the values between samples, in the Figures, the two impulses appear as two triangles. Also in the Figures, the two triangles are drawn symmetrically in the center of the plot. However, because we use an even number of samples, the diffraction-limited (DL) image is slightly asymmetrical. The number of samples used are more than it is required by Nyquist theorem. While the required number of Nyquist sample is unity here we use thirty-two samples. The oversampling is necessary because the impulses are not band-limited functions and also we wish to superresolve to closely spaced impulses.

In Fig. 1, the numerical instability of the pseudo-inverse matrix reconstructions, even in the absence of noise, is verified. Here the two impulses are separated by one-eighth of the Rayleigh distance. The solid curve represent the desired while the dotted curve represents the actual reconstruction. There is a factor of six compression on the numerical values of the dotted curve. Almost all traditional methods of regularization, even in the absence of noise, cannot resolve two impulses with Rayleigh spacing closer than one-half Rayleigh distance. In Fig. 2, smoothing in the eigen-value domain is introduced. The condition number, a measure of the rank of the H matrix, the ratio of the maximum to the minimum eigen-value is

reduced to one million. By fixing the condition number in this fashion, the eigen-values of H smaller than about 10^{-6} and the corresponding projected eigen-vectors are eliminated. Again the dotted curve is the reconstruction. While the reconstruction is smoother now as compared to the previous case, it still does not resolve the two impulses. If we are to reduce the condition number by a factor of a hundred (see Fig. 3), the reconstructed output is an even smoother than the previous case. However, the reconstruction is still not superresolving. In fact, all that the eigen-value filtering does is to produce a smoothed version of the DL image.

In Fig. 4, the effect of noise, rather than the eigen-value, filtering on the DL image is presented. Here the dotted curve represents the measured DL image while the solid curve represents the desired and the reconstructed image merged together. The spacing between the impulses is one eighth of a Rayleigh length. The only noise that has been added to the DL image is the unintentional truncation and propagation error, which are always present, that leaked into the computation. In this noise filtering scheme, the l_1 norm, both positive and negative going noise samples are allowed. The l_1 norm minimizes the linear sum of positive and negative noise samples. Note the perfect reconstruction of the triangular waveforms. If for the the conditions postulated in Fig. 4 a different noise filtering scheme is applied, see Fig. 5, the resulting reconstruction is not as faithful as in the previous case. Here the so-called minimax or l_∞ norm is used. This norm minimizes the largest noise sample value, be it positive of negative going. Fig. 5 indicates the critical effect of the reconstruction algorithm for an ill-conditioned system. It was initially thought that the noise statistics will have a critical role in choosing which type of optimal noise filter one should use. The difficulty of measuring the noise and the small sample population made the determination of the noise statistics an impossible choice.

For a realistic S/N the amount of superresolution must be curtailed. In general, it has been found that the achievable superresolution is a very sensitive function of the input S/N. While for high, and largely unrealistic S/N excellent superresolution is obtainable, using various type of noise filtering, once the S/N reaches realistic values catastrophic deterioration in the reconstructed image occurs. This problem is solved by the use of simultaneous linear eigen-value and noise filtering on DL image. The linear filtering smoothes the high spatial frequency, mainly noise, components of the DL image. There must be sufficient smoothing such that the optimal noise filter can accurately track the remaining lower spatial frequency components. In Fig. 6, the reconstruction of two impulses spaced one-half Rayleigh distance are shown. The rms noise component on the DL image is 0.1. This value of rms noise corresponds to an input S/N of 26 db. While this S/N is still rather high, to our knowledge even with this S/N, SIR has not been achieved. The amount of smoothing, the reduction of the condition number, has been adjusted experimentally. Note that the DL image has appreciable corners that must be smoothed. Even with this low S/N, the optimal l_1 noise filter shows perfect reconstruction. The minimax noise filter under identical conditions, see Fig. 7, has also the two impulses resolved. But there are additional artifacts generated in the reconstruction process. The S/N after processing is 24 db. The 2 db drop is the penalty we pay for the SIR. Finally, in Fig. 8, the input S/N is changed from 26 to 21 db. The reconstruction algorithm uses both linear and l_1 filtering. Note that the input DL image does not appreciable change from the previous case. However, the reconstructed image is not as faithful as in the previous case. The sample value in-between the impulses does not reach zero as it did in the previous case. Also, the output S/N drops by 7 db.

In summary, these figures show that a combination of linear eigen-filtering and linear programming techniques can result in SIR in a realistic noisy environment.

REFERENCES

1. B.R. Frieden, "Image Enhancement and Restoration", in Picture Processing and Digital Filtering, T.S. Huang, Ed., Springer-Verlag, New York, (1975).

2. S. Twomey, "The Application of Numerical Filtering to the Solution of Integral Equations Encountered in Indirect Sensing Measurements", J. Franklin, Inst., vol. 279, pp. 95-109 (1965).

3. J.P. Burg, "Maximum Entropy Spectral Analysis", presented at the 37th annual meeting of the Society of Exploration Geophysicists, Oklahoma City, Okla. (1967).

4. P.A. Jansson, R.H. Hunt, and E.K. Plyler, "Resolution Enhancement of Spectra", J. Opt. Soc. Am., 60, pp. 596-599 (1970).

5. A.C. Schnell, "Enhancing the Angular Resolution of Incoherent Sources", Radio Electron, Eng. 29, pp.21-26 (1965).

6. Y. Biraud, "A New Approach for Increasing the Resolving Power by Data Processing", Astron, Astrophys. 1, pp. 124-127 (1969).

7. D.L. Phillips, "A Technique for the Numerical Solution of Certain Integral Equations of the First Kind", J. Ass. Comput. Mach., vol. 9, pp. 84-96 (1962).

8. C.W. Helstrom, "Image Restoration by the Method of Least Squares", J. Opt. Soc. Am., vol. 57, pp. 297-303 (1967).

9. J.L. Harris, Sr., "Image Evaluation and Restoration", J. Opt. Soc. Am., vol. 56, pp. 569-574 (1966).

10. C.T. Baker, L. Fox, D.F. Mayers, K. Wright, "Numerical Solution of Fredholm Integral Equations of the First Kind", Comp. J., vol. 7, p. 141 (1964).

11. A.N. Tikhonov, "On the Solution of Incorrectly Posed Problems and the Method of Regularization", Soviet Math., vol. 4, pp. 1035-1038 (1963).

12a. D. Slepian and H.O. Polak, "Prolate Spheroidal Wave Functions, Fourier Analysis, and Uncertainty - I", Bell Syst. Tech. J. 40, pp. 43-63 (1961).

12b. D. Slepian, "Prolate Spheroidal Wave Functions, Fourier Analysis and Uncertainty - V: The discrete case", Bell Syst. Tech. J., vol. 57, pp. 1371-1430 (1978).

13. H.C. Andrews and B.R. Hunt, Digital Image Restoration, Prentice-Hall, Englewood Cliffs, N.J. (1977).

14. D.P. MacAdam, "Digital Image Restoration by Constrained Deconvolution", J. Opt. Soc. Am., vol. 60, pp. 1617-1627 (1970).

15. E.B. Barett, R.N. Devich, "Linear Programming Compensation for Space-variant Image Degradation", Proceedings SPIE/OSA Conf. on Image Processing, J.C. Urbach, Ed. Pacific Grove, California, vol. 74, pp. 152-158 (1976).

16. N.D.H. Mascarenhas and W.K. Pratt, "Digital Image Restoration Under a Regression Mode", IEEE Trans. Circuits and Systems, vol. CAS-22, pp. 252-266 (1975).

LIST OF CAPTIONS

Figure 1. Unconstrained SIR of two impulses spaced one-eighth of a Rayleigh distance apart. Only computer induced noise present. The dotted curve is the actual reconstruction scaled down by a factor of six. The solid curve is the desired image.

Figure 2. Constrained SIR of two impulses with condition number limited to one million. The dotted curve is the reconstruction. The solid curve is the desired image.

Figure 3. Constrained SIR of two impulses with condition number limited to one hundred thousand. The dotted curve is the reconstruction. The solid curve is the desired image.

Figure 4. Noiseless reconstruction of two impulses spaced one-eighth of a Rayleigh distance apart. Noise filter is an l_1 norm filter.

Figure 5. Noiseless reconstruction of two impulses spaced one-eighth of a Rayleigh distance apart. Noise filter is a minimax filter.

Figure 6. Reconstruction of two impulses one-half Rayleigh distance apart. The input waveform has a S/N of 26db. The input waveform has been eigen-value and noise filtered. The noise filter is l_1 norm filter.

Figure 7. Reconstruction of two impulses one-half Rayleigh distance apart. The input waveform has a S/N of 26db. The input waveform has been eigen-value and noise filtered. The noise filter is a minimax norm filter.

Figure 8. Reconstruction of two impulses one-half Rayleigh distance apart. The input waveform S/N is 21db. The input waveform has been eigen-value and noise-filtered. The noise filter is an L_1 filter.

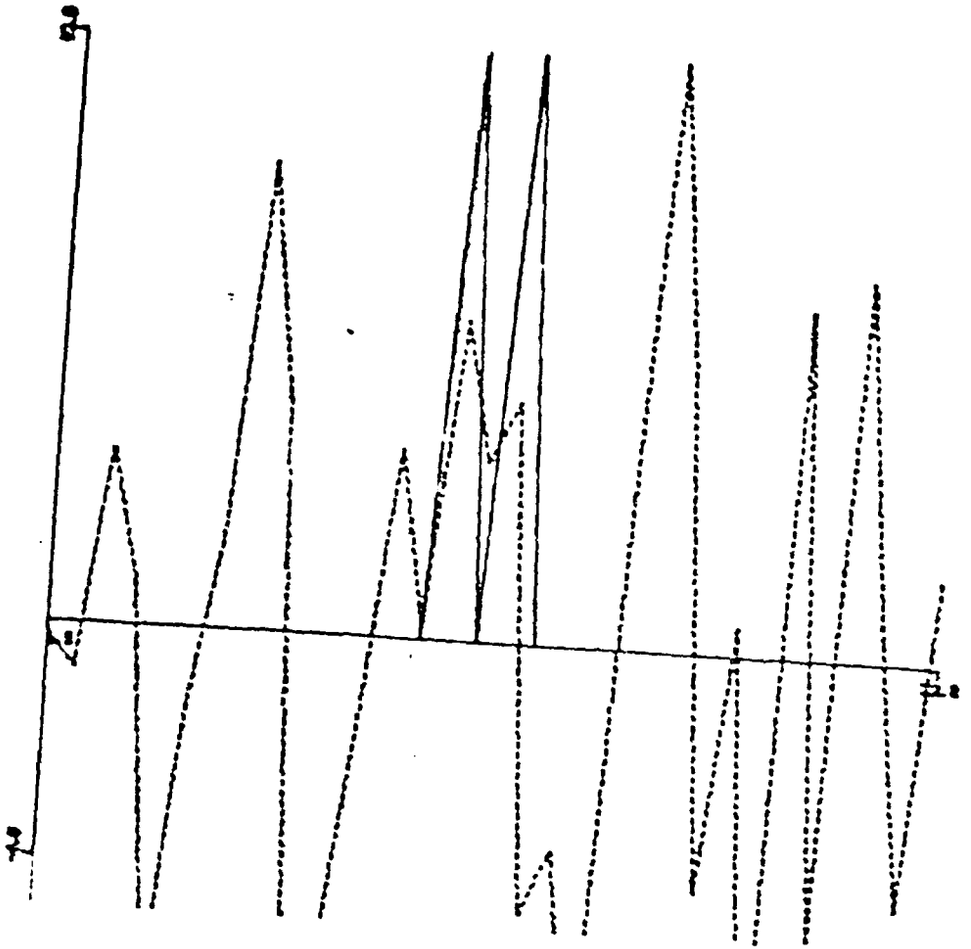

FIGURE 1

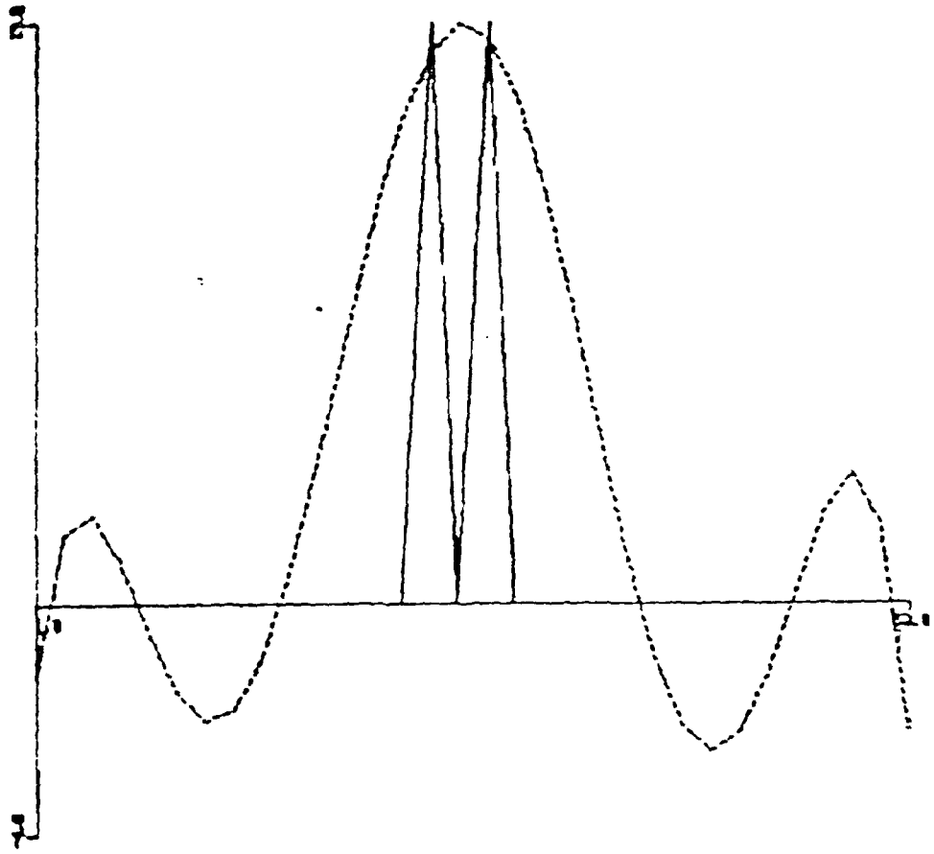

FIGURE 2

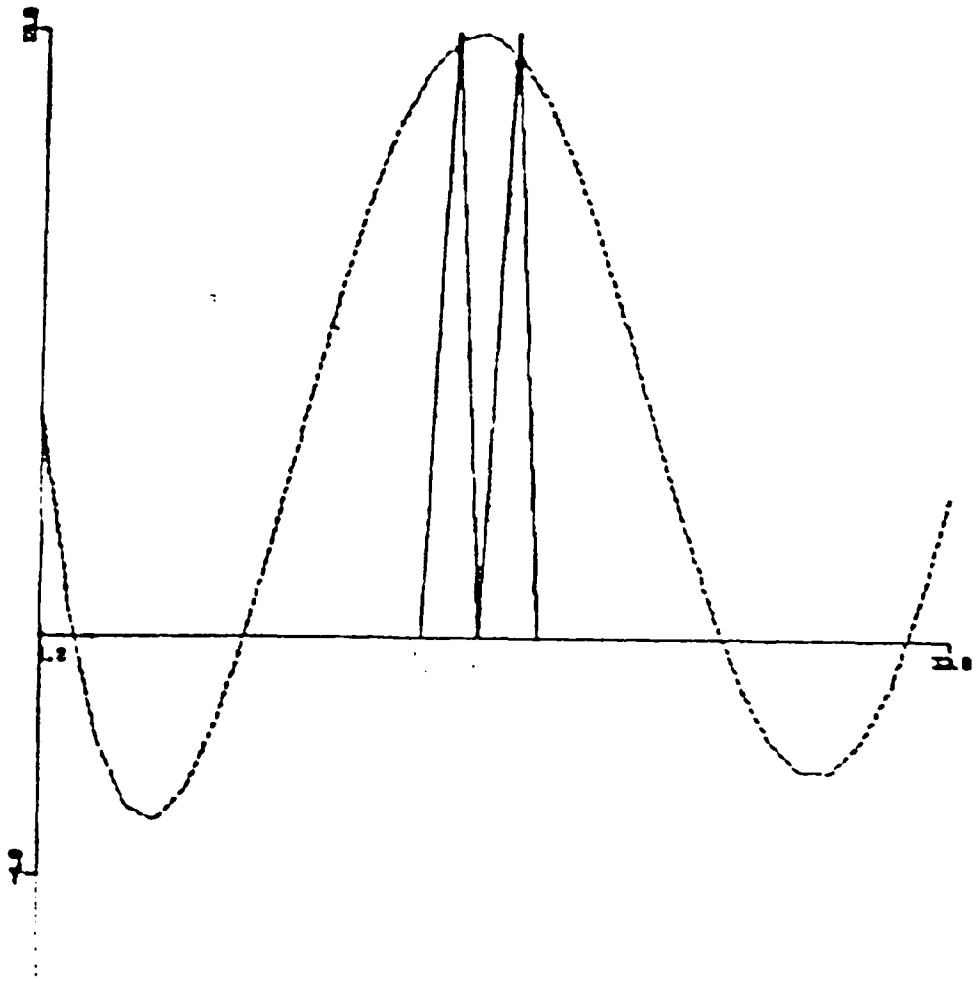

FIGURE 3

FIGURE 4

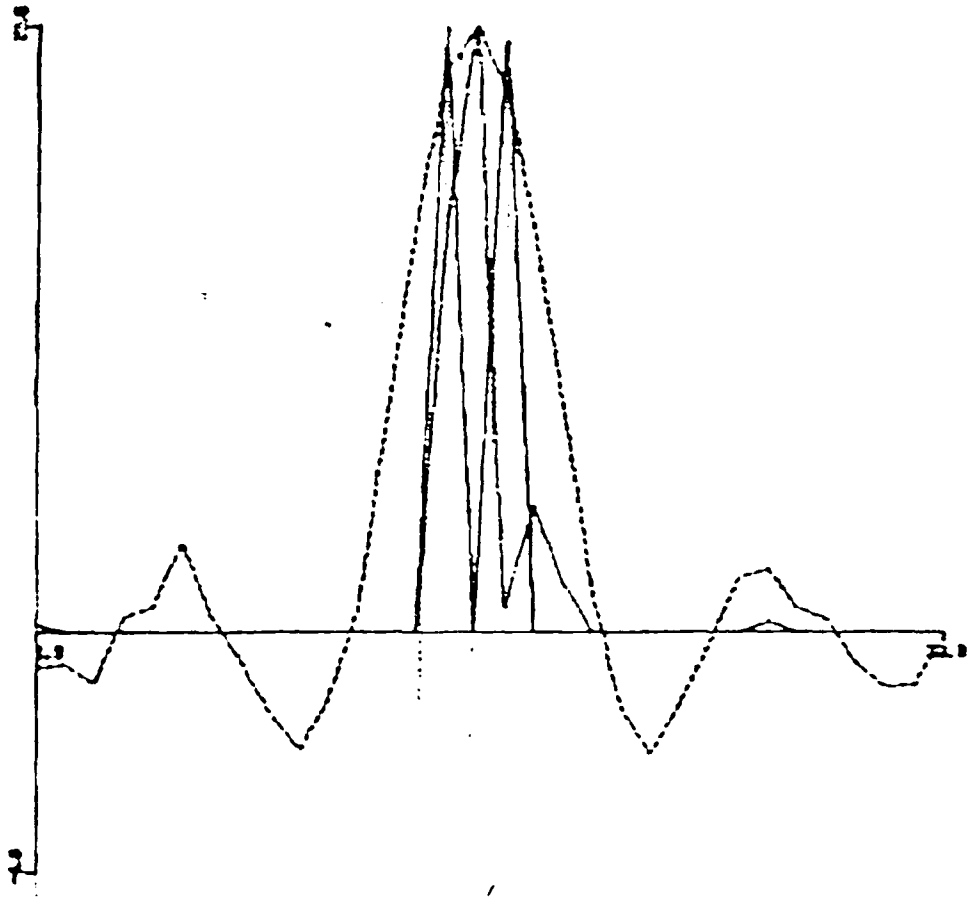

FIGURE 5

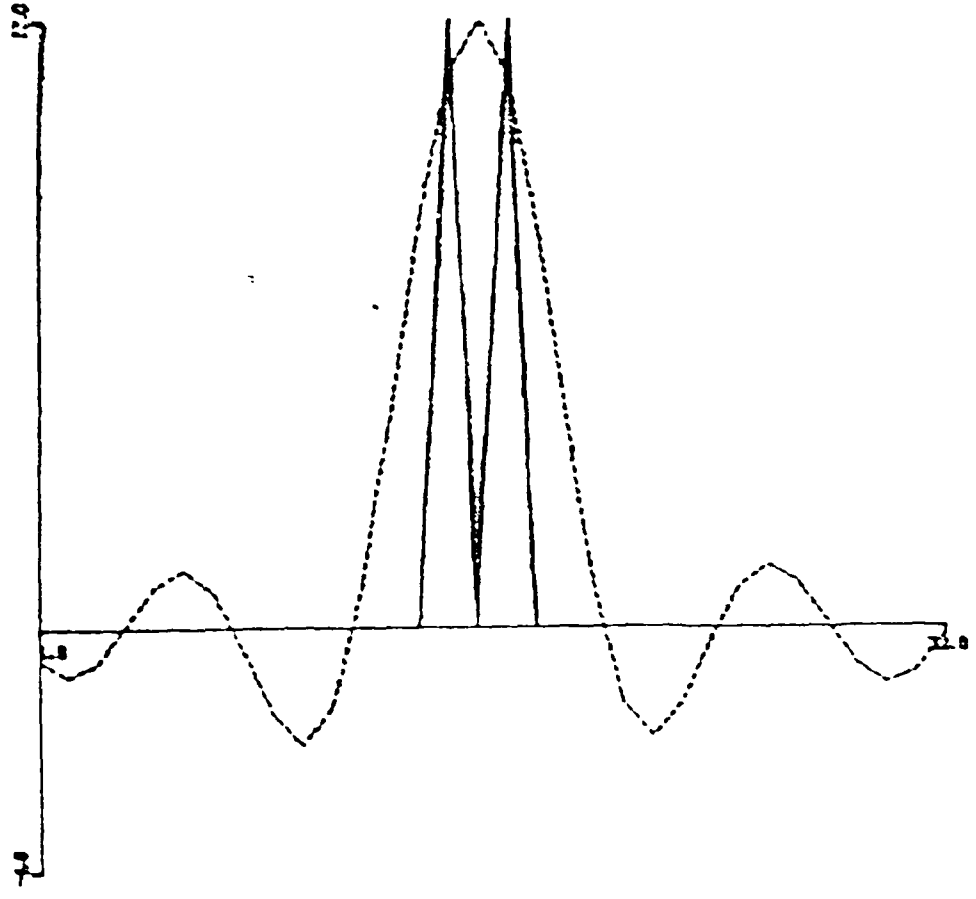

FIGURE 6

FIGURE 8

III. Professional Staff

1. Co-Principal Investigators

D. L. Schilling - Professor

G. Elchmann - Professor

T. Saadawi - Assistant Professor

2. Graduate Students

J. Cartwright

A. Fernandez

J. Keybl

R. Mammone

W. Moustakis

R. Stirbl

3. Undergraduate Students

S. Einbinder

S. Goldman

J. Londono

T. Manfre

J. Miranda

K. Nechamkin

M. Nicholson

E. Wallace

V. Youngatis

IV. Papers Published

1. G. Eichmann, R. Stirbl and J. Keybl, "Hybrid White-light video filtering for real-time digital still and moving color image transmission", JOSA, 70, p. 1589, 1980.

2. G. Eichmann and R. Mammone, "Optical image restoration of linearly degraded images", JOSA, 70, p. 1580, 1980.

3. M. Braff and D. L. Schilling, "The correlation of the output of a binary convolutional encoder", IEEE Trans. on Comm., Vol. COM-28, No. 3, March 1980.

4. D. L. Schilling, L. B. Milstein, and S. Davidovici, "The Effect of tone interfering signals on a direct sequence spread spectrum communication system, Submitted for Publication to IEEE Trans. on Communications.

END

DATE
FILMED

7-81

DTIC